

# Increased production of bacterial cellulose as starting point for scaled-up applications

Maria Gullo<sup>1</sup>  · Antonella Sola<sup>2</sup> · Gabriele Zanichelli<sup>1</sup> · Monia Montorsi<sup>3</sup> · Massimo Messori<sup>2</sup> · Paolo Giudici<sup>1</sup>

Received: 30 May 2017 / Revised: 13 September 2017 / Accepted: 18 September 2017 / Published online: 30 September 2017  
© Springer-Verlag GmbH Germany 2017

**Abstract** Bacterial cellulose is composed of an ultrafine nanofiber network and well-ordered structure; therefore, it offers several advantages when used as native polymer or in composite systems.

In this study, a pool of 34 acetic acid bacteria strains belonging to *Komagataeibacter xylinus* were screened for their ability to produce bacterial cellulose. Bacterial cellulose layers of different thickness were observed for all the culture strains. A high-producing strain, which secreted more than 23 g/L of bacterial cellulose on the isolation broth during 10 days of static cultivation, was selected and tested in optimized culture conditions. In static conditions, the increase of cellulose yield and the reduction of by-products such as gluconic acid were observed. Dried bacterial cellulose obtained in the optimized broth was characterized to determine its microstructural, thermal, and mechanical properties. All the findings of this study support the use of bacterial cellulose produced by the selected strain for biomedical and food applications.

**Keywords** Bacterial cellulose · *Komagataeibacter xylinus* · Strain selection · Biopolymer

## Introduction

Cellulose is the most abundant biopolymer on earth, and it is produced by plants, fungi, algae, and some bacterial species. It is composed of glucose monomers with  $\beta$ -1,4 glucosidic bonds. Although cellulose produced by different living organisms has identical chemical composition, bacterial cellulose (BC) has a peculiar supramolecular structure, and its bulk properties are different from those of cellulose produced by other organisms (Ross et al. 1991). BC is more pure than plant cellulose, because it does not contain hemicellulose or lignin, and it is composed of an ultrafine nanofiber network and well-ordered structure that offer several advantages when BC is used as native polymer or in composite systems. Moreover, the supramolecular structure of BC is responsible for the high water holding capacity, hydrophilic characteristic, and resistance to tensile strength (Cavka et al. 2013).

Recently, BC has received increasing attention because of its high potential in a wide array of applications such as healthy food, cosmetics, pharmaceutical and biomedical products, reinforcement of high-quality papers, diaphragms for electro-acoustic transducers, paint additives, coatings, reinforcement for optically transparent films, and proton-conducting membranes of fuel cells (Valera et al. 2015; Jiang et al. 2012; Gardner et al. 2008; Jonas and Farah 1998). Moreover, composites containing vegetal fibers have attracted a lot of attention due to the possibility of improving mechanical properties of the materials using a renewable resource, which generates a significantly lower level of environmentally dangerous gases as indicated by life cycle assessment studies (Ku et al. 2011). Obviously to promote the scale up of BC applications, the fundamental requirement is the high yield of production that is still a debated issue.

Several species of bacteria can produce BC, including the *Rhizobium*, *Agrobacterium*, and *Sarcina* genera and the acetic

✉ Maria Gullo  
maria.gullo@unimore.it

<sup>1</sup> Department of Life Sciences, University of Modena and Reggio Emilia, Via G. Amendola, 2, Pad. Besta, 42122 Reggio Emilia, Italy

<sup>2</sup> Department of Engineering “Enzo Ferrari”, University of Modena and Reggio Emilia, Via P. Vivarelli, 10, 41125 Modena, Italy

<sup>3</sup> Department of Sciences and Methods for Engineering, University of Modena and Reggio Emilia, Via G. Amendola 2, Pad. Morselli, 42122 Reggio Emilia, Italy

acid bacteria (AAB) group (Chawla et al. 2009). Within AAB, BC is produced by species of the genera *Acetobacter*, *Gluconacetobacter*, and *Komagataeibacter*. The strains that are recognized as the highest producers belong to the species *Komagataeibacter xylinus* (formerly *Gluconacetobacter xylinus*) which is considered the model organism in studies of BC synthesis (Benziman et al. 1980; Saxena et al. 1994). BC formation by *K. xylinus* is reported for several niches containing sugars and ethanol, such as fruits, vinegars, nata de coco, and Kombucha tea, where they develop on the surface of fermenting liquids and are entrapped in the exopolysaccharidic (EPS) matrix (Sievers et al. 1995; Giudici et al. 2009; Mamlouk et al. 2011; Semjonovs et al. 2017).

There is a large variation in the amount and yield of BC produced by different species and strains, and this is an important variable to consider, both for technological and scientific purposes. The yield of BC is also affected by the culture conditions such as the carbon source and the cultivation system. Glucose-based media alone or supplemented with other carbon sources (sucrose, fructose, maltose, glycerol, and xylose) and activators of BC synthesis have been studied extensively (Mikkelsen et al. 2009; Ramana et al. 2000; Son et al. 2001; Mamlouk and Gullo 2013; Hwang et al. 1999; Kuo et al. 2016; Yim et al. 2017). Moreover, low-cost feedstocks, such as wheat straw acid hydrolysate, lipid fermentation wastewater, and rotten apples, have been tested as alternative carbon sources (Hong et al. 2011; Huang et al. 2016; Park et al. 2003). These studies open new horizons for the industrial production of BC since they prove that low-cost feedstocks can significantly contribute to the reduction of production costs.

It is worth noting that BC synthesis is an energy-dependent process (Ross et al. 1991), and therefore, in a medium with only glucose as energy source, the oxidation of glucose to gluconate prevails over the synthesis of BC. Furthermore, the development of gluconate significantly decreases the pH of the medium and this is an additional limitation to the BC production. The addition of ethanol to glucose-containing media, as energy and carbon source, increases the BC yield because AAB preferentially use ethanol as energy source and glucose as carbon skeleton for building block and BC. Moreover, although AAB are tolerant to acetic acid at concentrations that are instead detrimental to the majority of microorganisms, a high amount of acetic acid (produced from ethanol) would be toxic for bacterial cells. The synthesis of BC is one of the protection mechanisms against acetic acid, since BC acts as a barrier to acetic acid reaching the cytoplasmic membrane of the cell (Kanchanarach et al. 2010; Gullo et al. 2014). The increased tolerance to acetic acid due to BC exerts a selective pressure on cellulose positive (Cel+) and negative (Cel-) mutants. While Cel+ mutants take advantage on Cel- ones in acetate media, the latter are favored in the absence of acetic acid. In addition, acetic acid can be used in the pathway of gluconeogenesis, increasing glucose availability (Velasco-Bedrán and López-Isunza 2007; Gullo et al. 2016).

The cultivation system strongly influences the yield and physical characteristics of BC. In static conditions, BC is thick and characterized by a well-defined reticulated structure. Although providing higher production rates of BC, agitated and air-forced systems show several disadvantages, including high frequency of cell mutants and the formation of sphere-like cellulose particles, an irregular form of BC in fibrous suspension, spheres, pellets, or irregular mass. Moreover, BC produced in agitated and aerated systems has lower crystallinity, mechanical strength, and degree of polymerization than that produced from static culture (Krystynowicz et al. 2002).

In this study, 34 AAB strains were screened for their ability to produce BC. Culture conditions were set up with the aim of increasing the BC production. In view of the possible future applications, the BC obtained by the selected strain was characterized to determine its microstructural features and thermomechanical properties.

## Materials and methods

### Bacterial strains

In this study, AAB strains previously isolated from different fractions (pellicle or liquid) of Kombucha tea were studied (Mamlouk 2012) (Table 1). Strains DSMZ 6513<sup>T</sup> (*K. xylinus*) and DSMZ 3503<sup>T</sup> (*Gluconobacter oxydans*) were obtained from DSMZ (Deutsche Sammlung von Mikroorganismen und Zellkulturen GmbH, Braunschweig, Germany) collection. Strain K2G30 was deposited at the Unimore Microbial Culture Collection (UMCC) under the collection number UMCC 2756.

### Culture conditions

The following media were used: GYC (10.0% glucose, 1.0% yeast extract (Oxoid Ltd., Basingstoke, UK), 2.0% calcium carbonate, dissolved in deionized water, pH not adjusted); when appropriate, agar (0.8%) was supplemented; GY (5.0% glucose, 1.0% yeast extract (Oxoid Ltd., Basingstoke, UK), dissolved in deionized water, pH not adjusted); GET (5.0% glucose, 0.1% yeast extract, 0.7% peptone (Oxoid Ltd., Basingstoke, UK), 0.8% disodium phosphate, 1.4% (v/v) ethanol dissolved in deionized water, pH not adjusted). The broths were sterilized at 121 °C for 15 min. Filtered (0.2 µm VWR International LLC, Radnor, USA) ethanol was added to GET broth after sterilization.

Pre-inocula for all experiments were prepared by transferring aliquots of cultures in the required broth. After 72 h of cultivation at 28 °C, tubes or flasks were vigorously shaken to remove cells embedded in the BC matrix, and the required amount of cell suspension was transferred.

**Table 1** Origin of strains used in this study and their growth modality

Strain	Isolation		Growth modality in liquid broth
	<i>Kombucha tea fraction</i>	<i>Fermentation time</i>	
K1G2	Liquid	<sup>a</sup> Pre-culture	EPS multilayer
K1G3	Liquid	Pre-culture	EPS single layer
K1G4	Liquid	0	EPS multilayer
K1G5	Liquid	0	EPS multilayer
K1G6	Liquid	0	EPS multilayer
K1G8	Liquid	3	EPS single layer
K1G22	Liquid	12	EPS multilayer
K1G23	Liquid	12	EPS single layer
K2G1	Liquid	Pre-culture	EPS multilayer
K2G2	Pellicle	Pre-culture	EPS multilayer
K2G5	liquid	Pre-culture	EPS single layer
K2G6	Liquid	Pre-culture	EPS multilayer
K2G8	Liquid	0	EPS single layer
K2G9	Liquid	0	EPS multilayer
K2G10	Liquid	0	EPS multilayer
K2G11	Liquid	0	EPS multilayer
K2G12	Liquid	0	EPS multilayer
K2G14	Liquid	0	EPS multilayer
K2G15	Liquid	0	EPS multilayer
K2G29	Pellicle	6	EPS single layer
K2G30	Pellicle	6	EPS multilayer
K2G31	Pellicle	6	EPS multilayer
K2G32	Liquid	6	EPS multilayer
K2G33	Liquid	6	EPS single layer
K2G34	Liquid	6	EPS single layer
K2G35	Liquid	6	EPS multilayer
K2G36	Liquid	6	EPS single layer
K2G37	Liquid	6	EPS single layer
K2G38	Liquid	6	EPS single layer
K2G39	Liquid	6	EPS single layer
K2G40	Liquid	6	EPS single layer
K2G41	Liquid	6	EPS single layer
K2G44	Liquid	12	EPS multilayer
K2G46	Liquid	12	EPS multilayer

<sup>a</sup> Pre-culture: previous Kombucha tea preparation used as inoculum

## Experimental procedure

AAB strains previously recovered from the selective BC source (Kombucha tea) were screened for their ability to synthesize BC by growing on GYC broth. BC yield of each strain was then determined after 10 days of static cultivation. The highest producing strain was tested on a larger scale (2.5-L vessel) using two different culture broths: GY broth and an optimized broth (GET), which was enriched

with ethanol as the second carbon source. This was done to determine the optimal culture condition to improve BC yield and reduce by-product formation.

BC obtained in the optimized broth was analyzed to determine its microstructural, thermal, and mechanical properties, as described in the following sections.

## Screening of strains for BC production

Culture strains were prepared from GYC pre-inocula and cultivated in aerobic conditions for 10 days at 28 °C. Qualitative BC production test was conducted by boiling pellicles recovered from culture broth in 4 mL of 5.0% NaOH solution for 2 h (Navarro et al. 1999). Strains of *K. xylinus* (DSM 6513) and *G. oxydans* (DSM 6513) were used as positive and negative controls, respectively. Tests were conducted in triplicate.

## BC production

The amount of BC produced in static conditions was determined in 100-mL flasks using GY broth (70 mL) and a pre-inoculum of 10 mL for each culture strain. For large-scale tests, the selected strain, according to the procedure described in the experimental procedure section, was used. Pre-inocula (300 mL) were prepared in GY and GET broths. Trials were conducted in vessels such as flasks, beakers, and containers of different sizes (0.500 to 2.5 L of capacity). The final test was performed in vessels (0.335 × 0.19 × 0.12 m) containing 2.5 L of the respective broths. Cultivation was carried out aerobically at 28 °C for 15 days. All the assays were conducted in duplicate.

## Purification and weighing of BC

The BC pellicle was collected from culture broth, washed twice or more times with distilled water, and then treated with 1% NaOH at 90 °C for 30 min. Treated BC was washed twice with distilled water, the pH of the residual water was determined, and washing was repeated until reaching neutral pH. Drying was conducted at 80 °C. BC weight was measured by analytical balance (Gibertini, Milan, Italy) (Hwang et al. 1999). Yield of BC produced was expressed in grams of dried BC per liter of broth and productivity in g/L/day.

The *BC yield on consumed sugar* (g/g) was calculated using the following equation:

$$BC \text{ yield on consumed sugar (g/g)} = \frac{BC \text{ yield (g)}}{Initial \text{ glucose (g)} - Final \text{ glucose (g)}} \quad (1)$$

## Analytic determination

D-glucose, D-gluconate, ethanol, and acetic acid were measured by enzymatic kits (Megazyme Ltd., Bray, Ireland) according to the manufacturer's instructions. pH was measured using an automatic titrator (TitroLine® EASY SCHOTT Instruments GmbH, Mainz, Germany), equipped with an SI Analytics electrode (SI Analytics, GmbH, Mainz, Germany).

## Characterization of BC produced by the selected strain in optimized conditions

The BC from the selected strain was characterized from microstructural, thermal, and mechanical viewpoints. To conduct the tests, fragments of appropriate size were excised from the dried BC membrane; alternatively, the dried BC was ground into powder by using a ceramic mortar and pestle at room temperature.

X-ray diffraction ("XRD", X'pert PRO, PANalytical, Almelo, the Netherlands) was conducted on a BC fragment (30 mm × 20 mm). Data were collected employing the CuK $\alpha$  radiation ( $\lambda = 1.54 \text{ \AA}$ ); the scans were processed in the angular range  $5^\circ$ – $60^\circ$   $2\theta$ , with a step size of  $0.008^\circ$   $2\theta$  and scan step time of 30.48 s.

The Fourier transform infrared spectroscopy ("FT-IR", FTIR VERTEX 70, Bruker Optik GmbH, Ettlingen, Germany) was carried out on a fragment working under the attenuated total reflection (ATR) mode, in the  $4000$ – $600 \text{ cm}^{-1}$  range.

The differential scanning calorimetry analysis ("DSC", TA DSC 2010, TA Instruments, New Castle, DE, USA) was performed on the BC powder. A single heating step was scheduled from  $-70$  to  $150 \text{ }^\circ\text{C}$  at a heating rate of  $+10 \text{ }^\circ\text{C min}^{-1}$  under nitrogen flow. More articulated tests implied multiple heating steps: the powder was heated from  $-70$  to  $+150 \text{ }^\circ\text{C}$  at  $+20 \text{ }^\circ\text{C min}^{-1}$ , cooled down from  $+150$  to  $-70 \text{ }^\circ\text{C}$  at  $-20 \text{ }^\circ\text{C min}^{-1}$ , and then heated again from  $-70$  to  $+150 \text{ }^\circ\text{C}$  at  $+20 \text{ }^\circ\text{C min}^{-1}$ .

The dynamic mechanical analysis ("DMA", TA DMA Q800, TA Instruments, New Castle, DE, USA) was focused on fragments, cut in the shape of  $30 \text{ mm} \times 10 \text{ mm}$  rectangles (thickness:  $20 \text{ }\mu\text{m}$ ). The tests were conducted in the film tension mode, working at a frequency of  $1 \text{ Hz}$ , an elongation of  $3 \text{ }\mu\text{m}$ , and a heating ramp from  $-60$  to  $+100 \text{ }^\circ\text{C}$  at  $3 \text{ }^\circ\text{C min}^{-1}$ . In addition, one fragment was tested as before, cooled down inside the closed furnace, and tested again according to the same parameters.

To measure the water absorption rate (W.A.R.),  $60 \text{ mm} \times 15 \text{ mm}$  rectangles were cut, dried at  $60 \text{ }^\circ\text{C}$  for 8 h, and weighted (dry mass,  $m_d$ ). The samples were then soaked

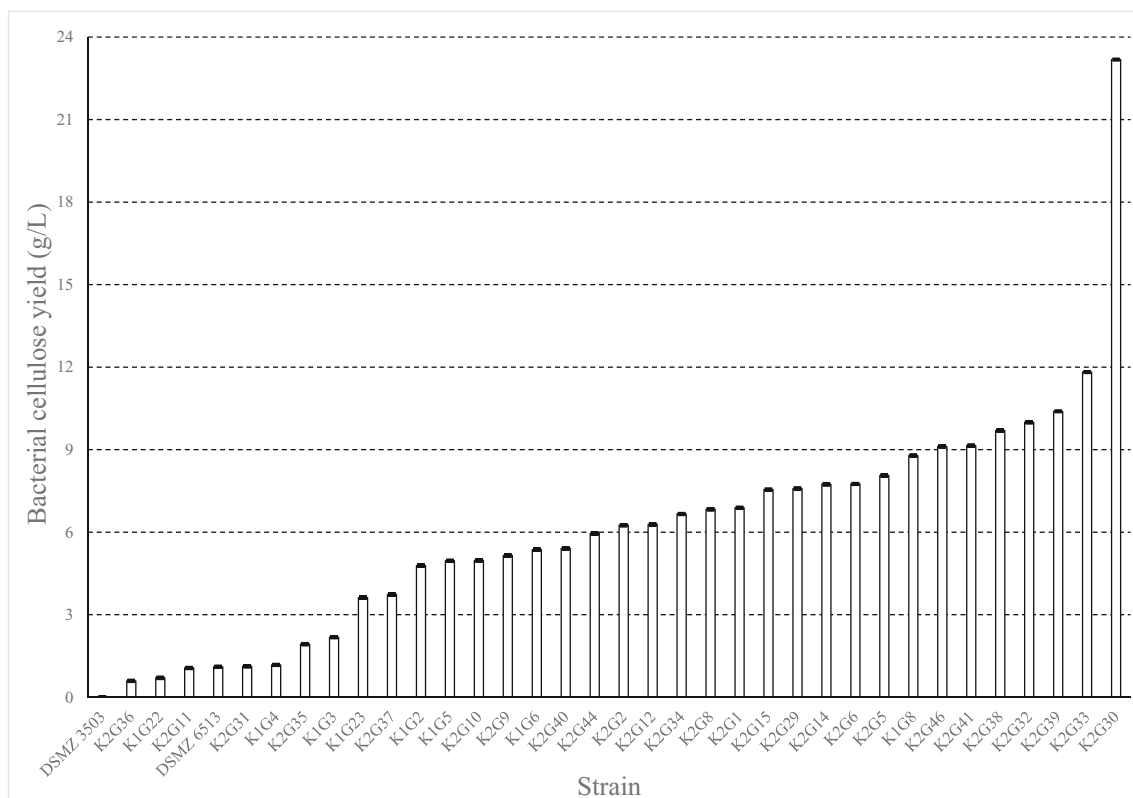


**Fig. 1** BC (g/L) produced by *K. xylinus* strains using 100 g/L of glucose as carbon source

in distilled water at room temperature for 48 h, gently dabbed with laboratory paper to remove the excess water on the surface, and weighted again (wet mass,  $m_w$ ). The W.A.R. (%) was calculated as:

$$W.A.R. = \frac{m_w - m_d}{m_d} \times 100 \quad (2)$$

## Results

### Screening for BC-producing strains

For all the strains, the growth modality in GYC broth after 4 days of cultivation differed from strain to strain. In fact, the thickness of the EPS layer formed on the surface of tubes was different and, for 20 strains, a multilayer formation was observed (Table 1). The nature of the produced EPS was first investigated on pellicles recovered from tubes. For all the strains, the EPS pellicle did not dissolve on boiling under 1% NaOH treatment, thus confirming to be BC.

### Selection of the highest cellulose producing strain

To determine the amount of BC synthesized, each strain was cultivated in flasks (100 mL) under static conditions at 28 °C for 10 days of incubation, using GYC broth. All the bacterial strains produced a BC layer of different thickness and appearance at the air–liquid interface of the culture broth. BC fraction required more than two washing steps to remove the calcium carbonate entrapped within the BC matrix, and it was then dried and weighted.

As shown in Fig. 1, BC production by *K. xylinus* strains ranged from 0 to 12 g/L with the only exception of strain K2G30 (isolated from the pellicle fraction of Kombucha tea after 6 days of fermentation), whose production (23 g/L) was sensibly higher. Therefore, K2G30 was chosen as the best BC producer and tested in optimized conditions.

### BC produced by K2G30 in optimized conditions

On the basis of the previous results and data reported in the literature (Hwang et al. 1999; Son et al. 2001), two broths were considered to further investigate BC production by the selected strain (K2G30) on a larger scale (2.50 L). A key point of the broth formulation was to reduce the amount of glucose, which was fixed at 50 g/L. Then, the following broths were tested: (1) a modified GYC broth (GY) in which calcium carbonate was removed and glucose reduced; (2) GET broth was formulated, which was composed of a double carbon source (glucose and ethanol), yeast extract, and peptone as nitrogen sources. After evaluating the suitability of GY and

GET broths in microscale conditions, which were conducted in test tubes for 10 days at 28 °C in static conditions, the larger-scale (2.50 L) cultivation was set up. The tests were conducted in vessels using static cultivation conditions. On the surface of the broths, after 2 days of incubation, a visible pellicle was formed, and it increased with time, reaching the maximum after 15 days. At the end of the cultivation process (15 days), the BC was collected, treated, and quantified; furthermore, the cultivation broths were analyzed to quantify residual compounds and formed by-products. The results clearly show that the BC production in GET was higher than in GY (Table 2). Native and dried BC produced by K2G30 are shown in Fig. 2a, b.

The yield of BC produced in GET and GY was generally higher than that reported in previous works conducted on AAB strains cultivated in similar conditions (Son et al. 2001; Hwang et al. 1999).

In this study, to maximize the BC production by K2G30, trials in vessels with different surface volume (S/V) ratios were performed (data not show). Finally, the 0.23 cm<sup>-1</sup> vessel was chosen according to the highest BC productivity and the lowest by-product formation (Table 2).

### Characterization of BC produced by the selected strain (K2G30) in optimized conditions

#### Composition and microstructure

The diffractogram of the BC fragment in Fig. 3 presents well-defined peaks situated at  $2\theta = 14.4^\circ$ ,  $2\theta = 16.8^\circ$ , and  $2\theta = 22.6^\circ$  that, according to the structural model proposed by Meyer, Mark, and Misch, can be associated to the crystal planes of type I native cellulose (Meyer and Mark 1928; Meyer and Misch 1937). In more detail, the cellulose under study, whose origin is bacterial, is expected to be of the  $I_\alpha$  type. To confirm this, the two equatorial d-spacings model proposed by Wada et al. (2001) can be applied. According to this approach, the two polymorphs can be differentiated using the function:

$$Z = 1693 d_1 - 902 d_2 - 549 \quad (3)$$

where  $d_1$  and  $d_2$ , are the (nominal) interplanar distances of the planes whose reflections generate the peaks at  $2\theta = 14.4^\circ$  and  $2\theta = 16.8^\circ$ , respectively, and where  $Z > 0$  if cellulose is prevalently of the  $I_\alpha$  type, while  $Z < 0$  if cellulose is prevalently of the  $I_\beta$  type (Wada et al. 2001). The interplanar distances calculated by the Bragg's equation for the diffractogram in Fig. 3 are  $d_1 = 0.613$  nm and  $d_2 = 0.526$  nm and, if such values are introduced in Eq. 2, it follows  $Z = 13.8 > 0$ , which confirms the cellulose under study is prevalently of the  $I_\alpha$  type, coherently with its bacterial origin (Wada et al. 2001). For completeness, also the value for  $d_3 = 0.393$  nm was calculated.

**Table 2** Carbon source consumption and bacterial cellulose production after 15 days of cultivation in vessel (S/V 0.23 cm<sup>-1</sup>)

Medium	pH		Glucose (g/L)		Ethanol (g/L)		Gluconic acid (g/L)	Acetic acid (g/L)	Bacterial cellulose (g/L)	Bacterial cellulose on consumed sugar (g/g)	Productivity (g/L × day)
	Initial	Final	Initial	Residual	Initial	Residual					
GY	5.40	3.14	50.00 ± 0.03	15.73 ± 0.03	0.00	0.00	22.23 ± 0.05	0.00	13.25 ± 1.11	0.39	0.88
GET	6.37	4.45	50.00 ± 0.02	18.00 ± 0.08	14.00 ± 0.05	2.20 ± 0.08	11.46 ± 0.05	0.67 ± 0.08	19.64 ± 0.94	0.61	1.3

The literature describes several approaches to estimate the degree of crystallinity (*d.o.c.*) of cellulose from its diffraction spectrum (Focher et al. 2001). Among them, *d.o.c.* can be calculated according to the Segal equation (Focher et al. 2001):

$$d.o.c. = \frac{I_{002} - I_{am}}{I_{002}} \times 100 \quad (4)$$

where  $I_{002}$  is the maximum intensity of the (002) lattice diffraction of type I cellulose (i.e., the intensity of the peak at  $2\theta = 22.6^\circ$ ), and  $I_{am}$  is the intensity diffraction at  $2\theta = 18^\circ$ , which is representative of the amorphous phase (Focher et al. 2001). The *d.o.c.* is therefore 80%.

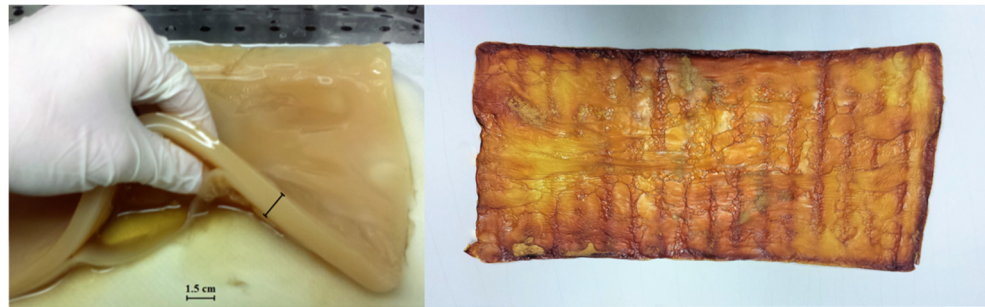
The FT-IR spectrum of a BC fragment is reported in Fig. 4. The peaks are typical for cellulose (Ul-Islam et al. 2013), apart from the strong signal at  $1600 \text{ cm}^{-1}$  that is instead due to absorbed water molecules, as frequently reported in the literature (Ul-Islam et al. 2013; Shablygin et al. 1972). Moreover, it is worth noting that the typical amid signals are missing due to the NaOH treatment to remove residues of cells and culture medium (Klemm et al. 2001). Generally speaking, no anomalous peaks appear in the spectrum, showing that the BC does not contain impurities (Semjonovs et al. 2017).

#### Thermal analysis

The DSC graph for the BC under investigation (powder sample) is shown in Fig. 5a. The outlined trend is coherent with the thermal behavior of BC described in the literature (Nada and Hassan 2000; Ciolacu and Popa 2006; Szcześniak et al. 2008). In more detail, the glass transition temperature,  $T_g$ , is situated at about  $0^\circ\text{C}$ ; then, if the temperature increases, a wide endothermic peak can be seen, which is due to the removal of the absorbed water (peak minimum at  $+80^\circ\text{C}$ ). The mass loss associated to the water removal, estimated by the difference in weight of the sample before and after heating, was 12.9%.

To study more extensively the thermal behavior, three-step DSC tests (heating–cooling–heating) were conducted, as shown in Fig. 5b. For the first heating step (heating (1), black solid line in Fig. 5b), the trend is the same as previously described for Fig. 5a; the glass transition temperature,  $T_{gH1} = +3^\circ\text{C}$ , and the endothermic peak, with a minimum at about  $98^\circ\text{C}$ , are slightly shifted to higher temperature values due to the higher heating rate (now,  $20^\circ\text{C min}^{-1}$  instead of  $10^\circ\text{C min}^{-1}$ ). While cooling in the subsequent step (green solid line in Fig. 5b), the detected glass transition temperature,  $T_{gC} = -9^\circ\text{C}$ , moves to slightly lower values due to the same “thermal inertia” effect. During the third step (heating (2), black dotted line in Fig. 5b), the glass transition temperature,  $T_{gH2} = +18^\circ\text{C}$ , is again slightly higher; most importantly, it is worth noting that the endothermic peak, although still present, is sensibly reduced with respect to the first heating step (heating (1) in Fig. 5b). This difference confirms that the endothermic peak is

**Fig. 2** Native (a) and dried (b) BC produced by K2G30 in GET broth during 15 days of cultivation



associated to the water removal, which mainly occurs during the first heating step (Szcześniak et al. 2008).

### Dynamic mechanical analysis

As shown in Fig. 6a, the storage modulus ( $E'$ ) of cellulose decreases as the temperature increases with a three-step process: at first, up to  $-20$  °C,  $E'$  remains almost unchanged, being very close to 5 GPa; then, between  $-20$  °C and  $+80$  °C,  $E'$  drops, while the damping factor ( $\tan \delta$ ) increases to maximum, which defines the DMA glass transition temperature  $T_{g\text{DMA}} = 28$  °C; finally, if the temperature increases further,  $E'$  remains close to 70 MPa.

The graphs acquired during two sequential heating steps are compared in Fig. 6b. The water loss caused by the first heating step (dotted lines in Fig. 6b) is responsible for the increase in the glass transition temperature, which, during the second heating step (solid lines in Fig. 6b), occurs over  $50$  °C, even if the broad shape of the  $\tan \delta$  peak does not allow defining univocally a single value for the glass transition temperature.

### W.A.R.

The W.A.R. after 48 h in distilled water is  $391 \pm 24\%$ . This value is comparable, for example, to that reported by Mohite and Patil (2014) for BC obtained from *K. hansenii* under dynamic conditions, despite the fact that the water absorption

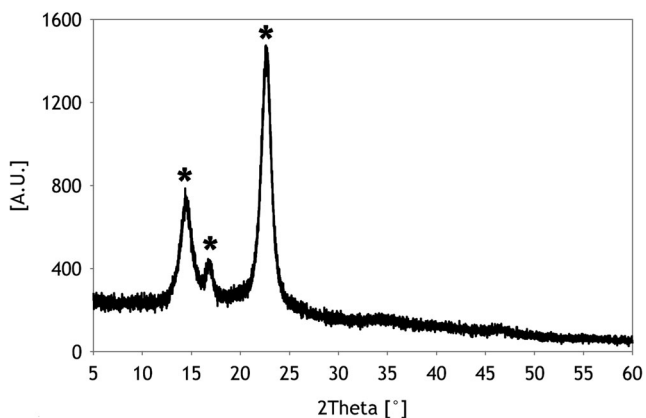


**Fig. 3** Diffractogram acquired on the BC membrane (fragment). The asterisk identifies the peaks of type I cellulose

capacity is usually higher for BC produced under dynamic conditions than for BC produced under static conditions.

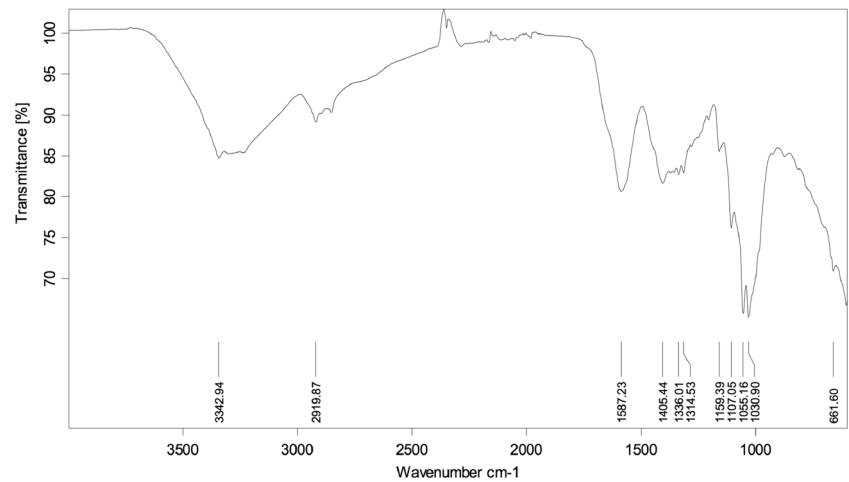
### Discussion

The results of this study showed that *K. xylinus* strain K2G30 is the highest BC producer among the tested strains, and it grew and maintained the ability to synthesize BC over preservation procedures. Since main traits such as BC and acetic acid syntheses can be lost due to preservation and cultivation cycles, the phenotypic stability check is a prerequisite for utilizing AAB in biotechnological processes (Gullo et al. 2012).

In the optimized conditions, the different production yields of BC in GY and GET broths by K2G30 could be due mainly to carbon sources and pH. When glucose was used as the sole carbon source (GY broth), 44.46% of the glucose was converted into gluconic acid as by-product. This percentage decreased to 22.92% of gluconic acid for GET broth containing glucose and ethanol as carbon sources. The formation of gluconic acid induced a decrease in pH, which dropped from 5.40 to 3.14 (GY) and from 6.37 to 4.45 (GET).

Gluconic and ketogluconic acids are the main metabolites of *K. xylinus* from glucose, which are involved in the pentose phosphate pathway during BC production. The formation of gluconic acid subtracts the carbon skeleton (glucose) from the BC production, and it exerts acidic stress on cells leading to depression of cell growth (Liu et al. 2016). Since the oxidation of glucose to gluconic acid and its derivatives is pH dependent (Cañete-Rodríguez et al. 2016; Giudici et al. 2016), some authors investigated the effect of pH on the yield of BC and gluconic acid synthesis by *K. xylinus*. However, there is no evidence for well-defined pH value to reach the maximum BC yield because it depends on a complex of factors (e.g., carbon source, cultivation system, pH) and, most of all, on the variability of each strain (Mikkelsen et al. 2009). Using glucose as the sole carbon source, the highest BC yield was obtained at pH 5.0, while at pH 4.0, the production of gluconic acid was higher than that observed at other pH values, and the production rate decreased with increasing pH (Hwang et al. 1999). In another study to maintain the pH in the optimal BC production range, an acetate-buffered medium (0.5% yeast extract, 0.5%

**Fig. 4** FT-IR spectra of the BC membrane (fragment)



peptone, and 6% glucose in acetate buffers of different pH and ionic strength) was used. The highest BC yield (7 g/L) was obtained when the pH shifted from an initial value of 4.75 to a final value of 3.86 (Kuo et al. 2016).

In this study, the second broth containing both glucose and ethanol, namely GET, was formulated because it has been previously proved that the addition of ethanol to glucose culture media significantly enhances BC production (Son et al. 2001; Krystynowicz et al. 2002). The trend of BC yield on consumed sugar increased from 0.39 g/g (GY) to 0.61 g/g (GET) (Table 2), confirming the evidence that ethanol acts as an additional energy source for ATP generation, allowing glucose to be used mainly for BC synthesis. Moreover, the residual acetic acid in GET broth after 15 days of cultivation was negligible, suggesting that it was metabolized via tricarboxylic acid cycle or that the formed oxaloacetate was decarboxylated into pyruvate that is used by the gluconeogenesis pathway to produce glucose, as previously stated for *K. xylinus* (Velasco-Bedrán and López-Isunza 2007). Gluconic acid production was twice lower than in GY and the higher pH values of GET broth favored the production of BC. Such results are consistent with previous studies showing that the highest BC production by *K. xylinus* strains is reached at pH > 4 whereas inhibition of the synthesis was observed at pH of 3.5–3.1 (Masaoka et al. 1993; Embuscado et al. 1994; Semjonovs et al. 2017).

In static cultivation, the aeration condition determined by the S/V ratio is an important factor affecting BC synthesis. In fact, it must be considered that, on the one hand, a larger culture area provides better surface aeration, thus increasing the dissolved oxygen in the broth that leads more glucose to be metabolized into gluconic acid, but, on the other hand, the BC production occurs at the air–liquid interface because of the higher oxygen availability, which implies that an increase in the S/V ratio also entails an enhancement of the BC production. In our study, the 0.23 cm<sup>-1</sup> vessel was chosen according to the highest BC productivity (1.3 g/L × day) and the lowest

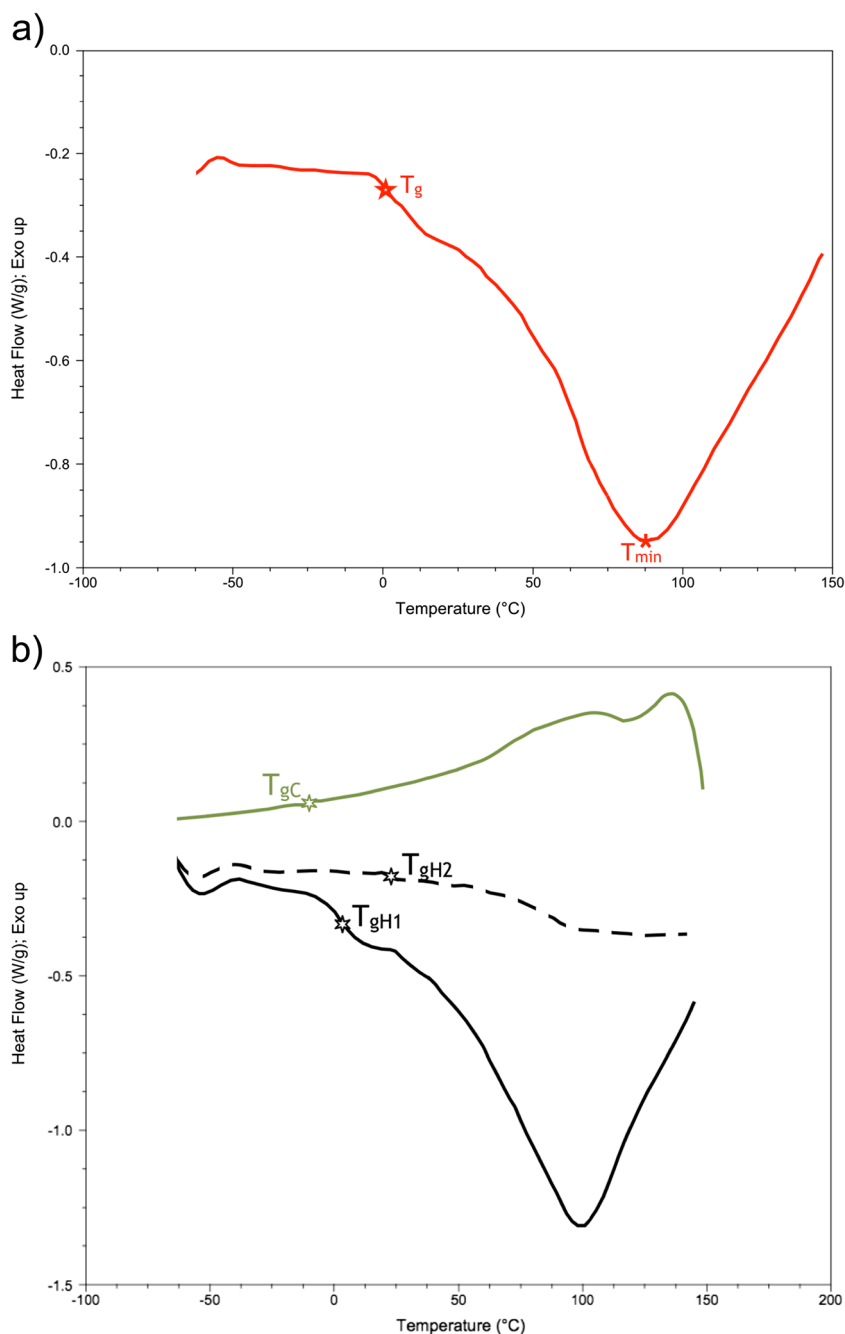
by-product formation (Table 2). The amount of BC produced (19.64 g/L) in these conditions was higher than that reported in earlier works. Krystynowicz and coworkers found that an S/V ratio of 0.71 cm<sup>-1</sup> facilitated the production of the highest amount of BC (3.5 g/L) by a *K. xylinus* strain (Krystynowicz et al. 2002). In another study, by culturing *K. xylinus* in four different-sized beakers, it was found that an S/V ratio of 0.55 cm<sup>-1</sup> was optimal to produce BC (7.23 g/L of BC with conversion yield of 0.2; 17.63 g/L of gluconic acid formed). When the S/V ratio increased to 1.31 cm<sup>-1</sup>, gluconic acid production was significantly increased to 41.55 g/L and the BC yield decreased correspondingly (Kuo et al. 2016).

The adoption of a high-producing AAB strain and the optimization of the cultivation conditions are essential in order to achieve the best BC productivity that is a prerequisite in view of an industrial scale-up. Besides, the use of low-cost feedstocks, such as by-products containing suitable carbon sources, seems promising for mass industrial production of BC (Hong et al. 2011; Huang et al. 2016; Park et al. 2003).

However, the exploitation of the BC membrane is also biased by its microstructural features and related thermomechanical properties. According to the quantitative analysis of the XRD results, the *d*-spacing values, which are associated to the structural characteristics of the BC crystallites, correspond well to other values reported in the literature. For example, Feng et al. (2015) focused on the BC membrane produced in static conditions by *K. hansenii* (strain 3917 CGMCC), which was mutated by high hydrostatic pressure treatment, and they obtained  $d_1 = 0.609$  nm,  $d_2 = 0.524$  nm, and  $d_3 = 0.391$  nm for the BC membrane dried by lyophilizer and  $d_1 = 0.602$  nm,  $d_2 = 0.522$  nm, and  $d_3 = 0.391$  nm for the BC membrane dried by oven. Analogously, Czaja et al. (2004) compared the structural characteristics of BC obtained in stationary and agitated culture by *K. xylinus* (strain NQ5) (Schramm–Hestrin medium) and they calculated  $d_1 = 0.602$  nm,  $d_2 = 0.523$  nm, and  $d_3 = 0.385$  nm for the BC sample from stationary cultivation; they also observed a decrease in the *d*-spacings for agitated culture conditions, probably as a



**Fig. 5** DSC thermograms of the BC powder, acquired by a single-step scan (a) and by a three-step scan (b). The latter implies heating (1), black solid line; cooling, green solid line; and heating (2), black dotted line. For both graphs: exothermic peaks upward

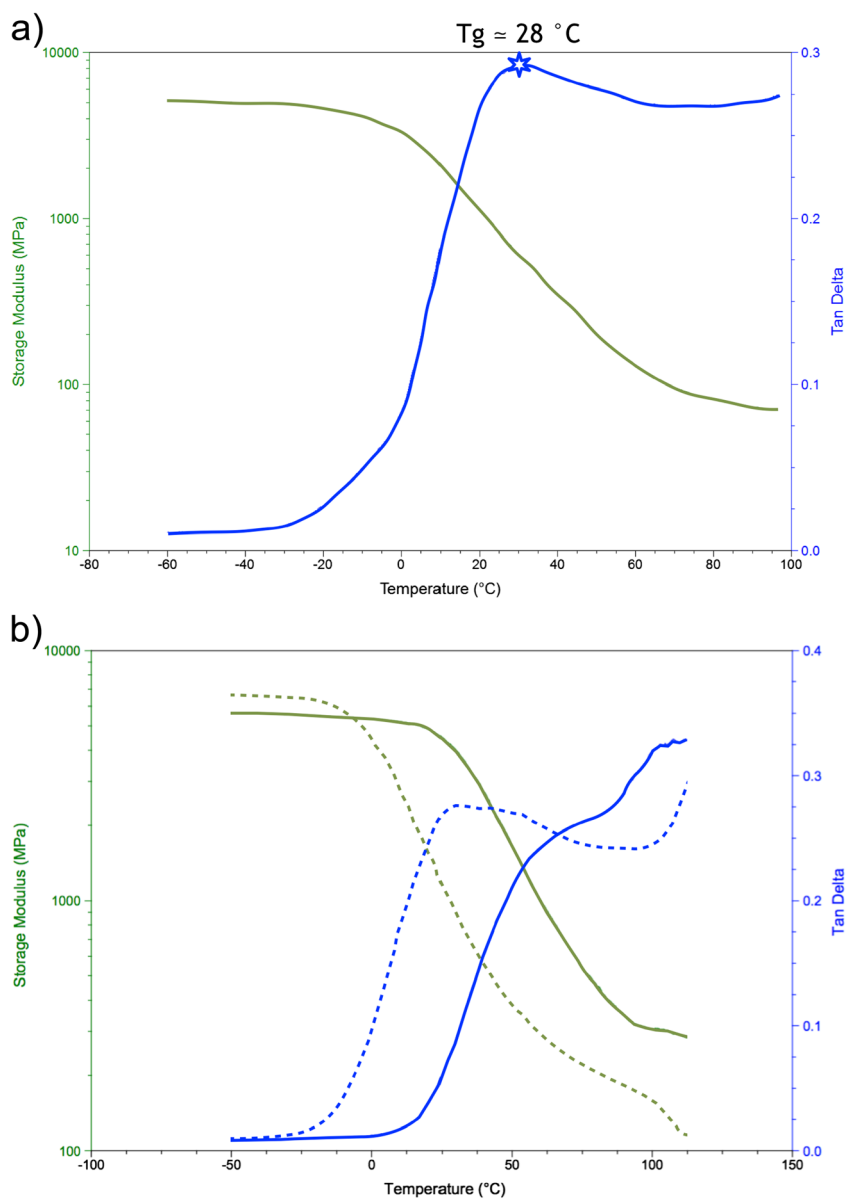


result of agitation-induced stresses that are likely to interfere with the crystallization process of nascent microfibrils.

Moreover, as proved by the diffractogram in Fig. 3, the BC produced by the K2G30 strain in optimized conditions is clearly of type  $I_\alpha$ . According to the model proposed by Atalla and Vanderhart (1989), native cellulose of type I is in fact the combination of two polymorphs, namely  $I_\alpha$  and  $I_\beta$ . In general, the two polymorphs coexist, but the relative amounts depend on the origin, since the  $I_\alpha$  prevails in cellulose produced by bacteria and algae whereas the  $I_\beta$  prevails in plant cellulose (Wada et al. 2001). Even if the debate is still open in the literature, the prevailing

presence of a specific polymorph affects the behavior of native cellulose, since cellulose  $I_\alpha$  is usually described as thermodynamically less stable and hence more reactive than cellulose  $I_\beta$  (Carlsson et al. 2015). In addition to polymorphism, also the crystallinity of BC affects its properties; in more detail, if the crystallinity increases, tensile strength, dimensional stability, and density are expected to increase, whereas chemical reactivity and swelling are expected to decrease. The analysis of the diffractogram in Fig. 3 yields  $d.o.c. = 80\%$ , which is emblematic of the high level of crystallization achieved by the BC under investigation. The highly crystalline structure of BC, together

**Fig. 6** DMA graphs of the BC membrane acquired by a single scan (a) and by a multiple scan (b) (first cycle, dotted lines; second cycle, solid line). For both graphs: in green, storage modulus,  $E'$  (y axis on the left side); in blue, damping factor,  $Tan \delta$  (y axis on the right side)



with its high purity, is one of the main reasons for its usage in several areas, including production of biomedical devices, stabilization of emulsions in cosmetic and food industry, immobilization of proteins, development of improved binders, design of stereo headphones and acoustic transducers, and reinforcement of paper (Jonas and Farah 1998, Yamanaka et al. 1989). Via selective hydrolyzation, highly pure and crystalline cellulose also represents a source of nanocrystals for advanced polymer-based composites (Zhou and Wu 2012).

In spite of its high *d.o.c.*, the dry BC membrane under investigation is able to absorb a relatively high amount of humidity, as proved by the decrease in weight (12.9%) associated to the water removal during the DSC. The progressive removal of water molecules, cycle by cycle, is likely to cause the observed increase in  $T_g$ , from  $T_{gH1} = +3\text{ °C}$  to  $T_{gH2} = +18\text{ °C}$  detectable in Fig. 5b. In

fact, water molecules bond to the polar groups of cellulose, thus weakening the forces between the glucose chains and increasing the free volume. As a consequence, if water molecules are removed, their plasticizing effect is reduced, and the glass transition occurs at higher temperature (Szakonyi and Zelkó 2012).

The plasticizing role of the absorbed water molecules clearly emerges from the multiple DMA tests in Fig. 6b, too. As a matter of fact, if the membrane is tested while heating, cooled down inside the furnace, and tested while heating again, the  $T_{gDMA}$  increases as a consequence of the removal of water molecules. Unfortunately, a direct comparison of the values for  $E'$  during the first and second heating cycles should be considered with caution, since the removal of the absorbed water modifies the original cross section of the sample, which is used by the software to calculate  $E'$ . However, as a rule, for

temperatures higher than 0 °C,  $E'$  is higher during the second cycle, because of the elimination of water (plasticizer). For temperatures below 0 °C, the trend is opposite, since  $E'$  is slightly higher during the first cycle. This is due to the presence, during the first cycle, of “freezable bound water” molecules (Szakonyi and Zelkó 2012) that, below 0 °C, are in the solid state (ice), thus contributing to the overall stiffness of the material, which correlates with its storage modulus.

Even if the impact of absorbed water molecules on the thermo-mechanical properties of the BC membrane must be kept into consideration, due to their obvious plasticizing effect, the high water absorption capacity ( $W.A.R.$ ) opens interesting possibilities for its usage. In fact, the ability to absorb and retain large amounts of water is one of the main reasons for applying cellulose as an additive in food (Shi et al. 2014) and, most importantly, as a bio-material (Gatenholm and Klemm 2010; Torres et al. 2012).

To conclude, the results of this study show that the highest BC yield was achieved by K2G30 strain in static cultivation using different culture broths. The optimal culture conditions included the formulation of a glucose/ethanol broth, which allowed to reduce the formation of gluconic acid and to maintain the pH in the range of 6.37–4.45. The BC produced by K2G30 in the optimized conditions possessed a high degree of crystallinity (about 80%). The abundant presence of absorbed water (about 12.9% for powdered BC) was responsible for the relatively low value of the glass transition temperature detected by the DSC analysis (about 0 °C). According to the DMA, the storage modulus remained almost unchanged up to –20 °C, being very close to 5 GPa; then, between –20 and +80 °C, the storage modulus gradually decreased to 70 MPa. The very high water absorption rate measured for the BC membrane ( $391 \pm 24\%$  in 48 h) supports its possible use in biomedical applications and in food processing.

Strain K2G30 is a high BC producer, and the BC synthesis seems stable over repeated cultivation cycles. This confirms the robustness of the strain and its suitability for further applications.

#### Compliance with ethical standards

**Ethical statement approval** This article does not contain any studies with human participants or animals performed by any of the authors.

**Conflict of interest** The authors declare that they have no conflict of interest.

#### References

- Atalla RH, Vanderhart DL (1989) Studies on the structure of cellulose using Raman spectroscopy and solid  $^{13}\text{C}$  NMR. In: Schuerch C (ed) Cellulose and wood: chemistry and technology, proceedings of the tenth cellulose conference. John Wiley and Sons, New York, NJ, U.S.A., pp 169–187
- Benziman M, Haigler CH, Brown RM Jr, White AR, Cooper KM (1980) Cellulose biogenesis: polymerization and crystallization are coupled processes in *Acetobacter xylinum*. Proc Natl Acad Sci U S A 77: 6678–6682
- Cañete-Rodríguez AM, Santos-Dueñas IM, Jiménez-Hornero JE, Ehrenreich A, Liebl W, García-García I (2016) Gluconic acid: properties, production methods and applications—an excellent opportunity for agro-industrial by-products and waste bio-valorization. Process Biochem 51:1891–1903. <https://doi.org/10.1016/j.procbio.2016.08.028>
- Carlsson DO, Lindh J, Strømme M, Mhryanyan A (2015) Susceptibility of  $\text{I}\alpha$ - and  $\text{I}\beta$ -dominated cellulose to TEMPO-mediated oxidation. Biomacromolecules 16:1643–1649. <https://doi.org/10.1021/acs.biomac.5b00274>
- Cavka A, Guo X, Tang SJ, Winestrand S, Jönsson L, Hong F (2013) Production of bacterial cellulose and enzyme from waste fiber sludge. Biotechnol Biofuels 6:25. <https://doi.org/10.1186/1754-6834-6-25>
- Chawla PR, Bajaj IB, Survase SA, Singhal RS (2009) Microbial cellulose: fermentative production and applications. Food Technol Biotech 47:107–124
- Ciolacu D, Popa VI (2006) On the thermal degradation of cellulose allomorphs. Cell Chem Technol 40:445–449
- Czaja W, Romanovicz D, Malcom Brown R (2004) Structural investigations of microbial cellulose produced in stationary and agitated culture. Cellulose 11:403–411. <https://doi.org/10.1023/B:CELL.0000046412.11983.61>
- Embuscado ME, Marks JS, Bemiller JN (1994) Bacterial cellulose. I. Factors affecting the production of cellulose by *Acetobacter xylinum*. Food Hydrocoll 8:407–418. [https://doi.org/10.1016/S0268-005X\(09\)80084-2](https://doi.org/10.1016/S0268-005X(09)80084-2)
- Feng X, Ullah N, Wang X, Sun X, Li C, Bai Y, Chen L, Li Z (2015) Characterization of bacterial cellulose by *Gluconacetobacter hansenii* CGMCC 3917. J Food Sci 80:E2217–E2227. <https://doi.org/10.1111/1750-3841.13010>
- Focher B, Palma MT, Canetti M, Torri G, Cosentino C, Gastaldi G (2001) Structural differences between non-wood plant celluloses: evidence from solid state NMR, vibrational spectroscopy and X-ray diffraction. Ind Crop Prod 13:193–208. [https://doi.org/10.1016/S0926-6690\(00\)00077-7](https://doi.org/10.1016/S0926-6690(00)00077-7)
- Gardner DJ, Oporto GS, Mills R, Azizi Samir MAS (2008) Adhesion and surface issues in cellulose and nanocellulose. J Adhes Sci Technol 22:545–567. <https://doi.org/10.1163/156856108X295509>
- Gatenholm P, Klemm D (2010) Bacterial nanocellulose as a renewable material for biomedical applications. MRS Bull 35:208–213. <https://doi.org/10.1557/mrs2010.653>
- Giudici P, De Vero L, Gullo M, Solieri L, Lemmetti F (2016) Fermentation strategy to produce high gluconate vinegar. Acetic Acid Bact 5:6067. <https://doi.org/10.4081/aab.2016.6067>
- Giudici P, Gullo M, Solieri L, Falcone PM (2009) Technological and microbiological aspects of traditional balsamic vinegar and their influence on quality and sensorial properties. Adv Food Nutr Res 58:137–182. [https://doi.org/10.1016/S1043-4526\(09\)58004-7](https://doi.org/10.1016/S1043-4526(09)58004-7)
- Gullo M, Mamlouk D, De Vero L, Giudici P (2012) *Acetobacter pasteurianus* strain AB0220: cultivability and phenotypic stability over 9 years of preservation. Curr Microbiol 64:576–580. <https://doi.org/10.1007/s00284-012-0112-9>
- Gullo M, Verzelloni E, Canonico M (2014) Aerobic submerged fermentation by acetic acid bacteria for vinegar production: process and biotechnological aspects. Process Biochem 49:1571–1579. <https://doi.org/10.1016/j.procbio.2014.07.003>
- Gullo M, Zanichelli G, Verzelloni E, Lemmetti F, Giudici P (2016) Feasible acetic acid fermentations of alcoholic and sugary substrates in combined operation mode. Process Biochem 51:1129–1139. <https://doi.org/10.1016/j.procbio.2016.05.018>
- Hong F, Zhu YX, Yang G, Yang XX (2011) Wheat straw acid hydrolysate as a potential cost-effective feedstock for production of bacterial

- cellulose. *J Chem Technol Biotechnol* 86:675–680. <https://doi.org/10.1002/jctb.2567>
- Huang C, Guo H, Xiong L, Wang B, Shi S, Chen X, Lin X, Wang C, Luo J, Chen X (2016) Using wastewater after lipid fermentation as substrate for bacterial cellulose production by *Gluconacetobacter xylinus*. *Carbohydr Polym* 136:198–202. <https://doi.org/10.1016/j.carbpol.2015.09.043>
- Hwang JW, Yang YK, Hwang JK, Pyun YR, Kim YS (1999) Effects of pH and dissolved oxygen on cellulose production by *Acetobacter xylinum* BRC5 in agitated culture. *J Biosci Bioeng* 88:183–188. [https://doi.org/10.1016/S1389-1723\(99\)80199-6](https://doi.org/10.1016/S1389-1723(99)80199-6)
- Jiang G, Qiao J, Hong F (2012) Application of phosphoric acid and phytic acid doped bacterial cellulose as novel proton-conducting membranes to PEMFC. *Int J Hydrog Energy* 37:9182–9192. <https://doi.org/10.1016/j.ijhydene.2012.02.195>
- Jonas R, Farah LF (1998) Production and application of microbial cellulose. *Polym Degrad Stabil* 59:101–106. [https://doi.org/10.1016/S0141-3910\(97\)00197-3](https://doi.org/10.1016/S0141-3910(97)00197-3)
- Kanchanarach W, Theeragool G, Inoue T, Yakushi T, Adachi O, Matsushita K (2010) Acetic acid fermentation of *Acetobacter pasteurianus*: relationship between acetic acid resistance and pellicle polysaccharide formation. *Biosci Biotechnol Biochem* 74:1591–1597. <https://doi.org/10.1271/bbb.100183>
- Klemm D, Schumann D, Udhardt U, Marsch S (2001) Bacterial synthesized cellulose- artificial blood vessels for microsurgery. *Prog Polym Sci* 26:1561–1603. [https://doi.org/10.1016/S0079-6700\(01\)00021-1](https://doi.org/10.1016/S0079-6700(01)00021-1)
- Krystynowicz A, Czaja W, Wiktorowska-Jeziarska A, Gonçalves-Miśkiewicz M, Turkiewicz M, Bielecki S (2002) Factors affecting the yield and properties of bacterial cellulose. *J Ind Microbiol Biotechnol* 29:189–195. <https://doi.org/10.1038/sj.jim.7000303>
- Ku H, Wang H, Pattarachaiyakop N, Trada M (2011) A review on the tensile properties of natural fiber reinforced polymer composites. *Compos Part B Eng* 42:856–873. <https://doi.org/10.1016/j.compositesb.2011.01.010>
- Kuo CH, Chen JH, Liou BK, Lee CK (2016) Utilization of acetate buffer to improve bacterial cellulose production by *Gluconacetobacter xylinus*. *Food Hydrocoll* 53:98–103. <https://doi.org/10.1016/j.foodhyd.2014.12.034>
- Liu M, Zhong C, Zhang YM, Xu ZM, Qiao CS, Jia SR (2016) Metabolic investigation in *Gluconacetobacter xylinus* and its bacterial cellulose production under a direct current electric field. *Front Microbiol* 7:331. <https://doi.org/10.3389/fmicb.2016.00331>
- Mamlouk D (2012) Insight into physiology and functionality of acetic acid bacteria through a multiphasic approach. Dissertation, University of Modena and Reggio Emilia, Reggio Emilia, Italy
- Mamlouk D, Gullo M (2013) Acetic acid bacteria: physiology and carbon sources oxidation. *Indian J Microbiol* 53:377–384. <https://doi.org/10.1007/s12088-013-0414-z>
- Mamlouk D, Hidalgo C, Torija MJ, Gullo M (2011) Evaluation and optimisation of bacterial genomic DNA extraction for no-culture techniques applied to vinegars. *Food Microbiol* 28:1374–1379. <https://doi.org/10.1016/j.fm.2011.06.009>
- Masaoka S, Ohe T, Sakota N (1993) Production of cellulose from glucose by *Acetobacter xylinum*. *J Ferment Bioeng* 75:18–22. [https://doi.org/10.1016/0922-338X\(93\)90171-4](https://doi.org/10.1016/0922-338X(93)90171-4)
- Meyer KH, Mark H (1928) Über den Bau des krystallisierten Anteils der Cellulose. *Ber Dtsch Chem Ges* 61(B):593–614. <https://doi.org/10.1002/cber.19280610402>
- Meyer KH, Misch L (1937) Positions des atomes dans le nouveau modele spatial de la cellulose. *Helv Chim Acta* 20:232–245. <https://doi.org/10.1002/hlca.19370200134>
- Mikkelsen D, Flanagan BM, Dykes GA, Gidley MJ (2009) Influence of different carbon sources on bacterial cellulose production by *Gluconacetobacter xylinus* strain ATCC 53524. *J Appl Microbiol* 107:576–583. <https://doi.org/10.1111/j.1365-2672.2009.04226.x>
- Mohite BV, Patil SV (2014) Physical, structural, mechanical and thermal characterization of bacterial cellulose by *G. hansenii* NCIM 2529. *Carbohydr Polym* 106:132–141. <https://doi.org/10.1016/j.carbpol.2014.02.012>
- Nada AMA, Hassan ML (2000) Thermal behavior of cellulose and some cellulose derivatives. *Polym Degrad Stab* 67:111–115. [https://doi.org/10.1016/S0141-3910\(99\)00100-7](https://doi.org/10.1016/S0141-3910(99)00100-7)
- Navarro RR, Sumi K, Matsumura M (1999) Improved metal affinity of chelating adsorbents through graft polymerization. *Water Res* 33:2037–2044. [https://doi.org/10.1016/S0043-1354\(98\)00421-7](https://doi.org/10.1016/S0043-1354(98)00421-7)
- Park JK, Park YH, Jung JY (2003) Production of bacterial cellulose by *Gluconacetobacter hansenii* PJK isolated from rotten apple. *Biotechnol Bioprocess Eng* 8:83–88. <https://doi.org/10.1007/BF02940261>
- Ramana KV, Tomar A, Singh L (2000) Effect of various carbon and nitrogen sources on cellulose synthesis by *Acetobacter xylinum*. *World J Microbiol Biotechnol* 16:245–248. <https://doi.org/10.1023/A:1008958014270>
- Ross P, Mayer R, Benziman M (1991) Cellulose biosynthesis and function in bacteria. *Microbiol Rev* 55:35–58
- Saxena IM, Kudlicka K, Okuda K, Brown RM Jr (1994) Characterization of genes in the cellulose-synthesizing operon (acs operon) of *Acetobacter xylinum*: implications for cellulose crystallization. *J Bacteriol* 176:5735–5752. <https://doi.org/10.1128/jb.176.18.5735-5752.1994>
- Semjonovs P, Ruklisha M, Paegle L, Saka M, Treimane R, Skute M, Rozenberga L, Vikele L, Sabovics M, Cleenwerck I (2017) Cellulose synthesis by *Komagataeibacter rhaeticus* strain P 1463 isolated from Kombucha. *Appl Microbiol Biotechnol* 101:1003–1012. <https://doi.org/10.1007/s00253-016-7761-8>
- Shablygin MV, Nikitina OA, Sokolova SA, Mikhailov NV (1972) Method of assessment of the effect of water on IR spectra of cellulose. *Polym Sci USSR* 14:2644–2648. [https://doi.org/10.1016/0032-3950\(72\)90427-3](https://doi.org/10.1016/0032-3950(72)90427-3)
- Shi Z, Zhang Y, Phillips GO, Yang G (2014) Utilization of bacterial cellulose in food. *Food Hydrocoll* 35:539–545. <https://doi.org/10.1016/j.foodhyd.2013.07.012>
- Sievers M, Lanini C, Weber A, Schuler-Schmid U, Teuber M (1995) Microbiology and fermentation balance in a Kombucha beverage obtained from a tea fungus fermentation. *Syst Appl Microbiol* 18:590–594. [https://doi.org/10.1016/S0723-2020\(11\)80420-0](https://doi.org/10.1016/S0723-2020(11)80420-0)
- Son HJ, Heo MS, Kim YG, Lee SJ (2001) Optimization of fermentation conditions for the production of bacterial cellulose by a newly isolated *Acetobacter*. *Biotechnol Appl Biochem* 33:1–5. <https://doi.org/10.1042/BA20000065>
- Szakonyi G, Zelkó R (2012) The effect of water on the solid state characteristics of pharmaceutical excipients: molecular mechanisms, measurement techniques, and quality aspects of final dosage form. *Int J Pharm Investig* 2:18–25. <https://doi.org/10.4103/2230-973X.96922>
- Szcześniak L, Rachocki A, Tritt-Goc J (2008) Glass transition temperature and thermal decomposition of cellulose powder. *Cellulose* 15:445–451. <https://doi.org/10.1007/s10570-007-9192-2>
- Torres FG, Commeaux S, Troncoso OP (2012) Biocompatibility of bacterial cellulose based biomaterials. *J Funct Biomater* 3:864–878. <https://doi.org/10.3390/jfb3040864>
- Ul-Islam M, Ha JH, Khan T, Park JK (2013) Effects of glucuronic acid oligomers on the production, structure and properties of bacterial cellulose. *Carbohydr Polym* 92:360–366. <https://doi.org/10.1016/j.carbpol.2012.09.060>
- Valera MJ, Torija MJ, Mas A, Mateo E (2015) Cellulose production and cellulose synthase gene detection in acetic acid bacteria. *Appl Microbiol Biotechnol* 99:1349–1361. <https://doi.org/10.1007/s00253-014-6198-1>
- Velasco-Bedrán H, López-Isunza F (2007) The unified metabolism of *Gluconacetobacter entanii* in continuous and batch processes. *Process Biochem* 42:1180–1190. <https://doi.org/10.1016/j.procbio.2007.05.017>

- Wada M, Okano T, Sugiyama J (2001) Allomorphs of native crystalline cellulose I evaluated by two equatorial d-spacings. *J Wood Sci* 47: 124–128. <https://doi.org/10.1007/BF00780560>
- Yamanaka S, Watanabe K, Kitamura N, Iguchi M, Mitsuhashi S, Nishi Y, Uryu M (1989) The structure and mechanical properties of sheets prepared from bacterial cellulose. *J Mater Sci* 24:3141–3145. <https://doi.org/10.1007/BF01139032>
- Yim SM, Song JE, Kim HR (2017) Production and characterization of bacterial cellulose fabrics by nitrogen sources of tea and carbon sources of sugar. *Process Biochem*. <https://doi.org/10.1016/j.procbio.2016.07.001>
- Zhou C, Wu Q (2012) Recent development in applications of cellulose nanocrystals for advanced polymer-based nanocomposites by novel fabrication strategies. In: Neralla S (ed) *Nanocrystals—synthesis, characterization and applications*, InTech, Rijeka, Croatia. <https://doi.org/10.5772/48727>